COO-4246-10

MICROSTRUCTURAL EFFECTS IN ABRASIVE WEAR

Quarterly Progress Report
for the period 15 July 1979 - 15 September 1979

Nicholas F. Fiore and Thomas H. Kosel

Department of Metallurgical Engineering and Materials Science
Notre Dame, IN 46556

15 October 1979

Prepared for

U. S. Department of Energy

Under Contract No. EF-77-S-02-4246

DISCLAIMER

ABSTRACT

The objective of this research program is to establish quantitative relations between microstructure and wear resistance of highly alloyed materials, including high-Cr white irons and experimental Co-base and Ni-base powder metallurgy (PM) alloys now used or potentially to be used in coal mining, handling and gasification. The specific types of wear under study are low-stress abrasion, encountered in coal conversion and transfer applications, and gouging wear encountered in mining. The objective has two facets. On the practical side, the establishment of the optimum microstructures for wear resistance will allow design engineers to make more effective decisions regarding candidate alloys for coal-conversion processes. On the basic side, the establishment of a better understanding of the physical and mechanical metallurgy of wear will allow development of alloys with maximum wear resistance in a specific application with minimum alloy content.

The project has been in existence for 27 months, and has just been renewed for an additional 24 months. During the first 27 months (Phase I), research was conducted on existing alloy cast irons from the ASTM 532 series and existing Co-base PM alloys. In Phase II of the work, research will be conducted on experimental cast irons, Ni-base and Co-base alloys which show potential for providing extremely good abrasion resistance while containing substantially less alloy content than existing materials. In this first quarter of Phase II, the analysis of the Phase I Co-base results has been completed and two of the four sets of experimental alloys have been obtained.

CONTENTS

1. OBJECTIVE AND SCOPE

1.1 Background

This project has been in existence for about two and one-half years, and has been renewed for an additional two years. This report is the 10th in a series of quarterly reports which summarize the research conducted.

In very general terms, the purpose of this project is to develop quantitative relations between microstructure and abrasion resistance of highly alloyed white irons and Co- and Ni-base powder metallurgy (PM) alloys commonly used in coal conversion processes. The research includes study of gouging wear resistance, necessary in mining operations, and low-stress abrasion resistance required in coal and coal-product handling and transfer operations. The project has both applied and basic aspects. On the applied side, the establishment of the optimum microstructures for wear resistance is allowing design engineers to make more effective decisions regarding candidate alloys for coal-related processes. From the basic viewpoint, the establishment of a better understanding of the physical and mechanical metallurgy of wear is the foundation for the long-range development of more economical and effective wear-resistant alloys.

In this first two and one-half years of the work (Phase I), effort has been concentrated on the study of abrasion resistance in a spectrum of existing white irons (ASTM Series 532) and Co-base alloys. Phase II of the work will involve the study of wear in irons of low Cr content and in Ni-base as well as Co-base PM alloys; thus this phase adds to the basic and applied aspects of the project the aspect of conservation of strategic alloying elements. The aspect of the work is being conducted in close cooperation with alloy producers (Climax Molybdenum Corporation and Stellite-Cabot Corporation), who are in the process of developing less expensive alloys for wear resistance. Phase II of the project follows directly from Phase I, and a summary of results achieved in the first phase is given in the following

section of this report.

1.2 Summary of Phase I

1.2.1 Scope

Phase I involved the study of standard alloy white irons and Co-base PM alloys. The work was based on a three-way experimental program consisting of mechanical testing, metallographic analysis and wear testing. The mechanical testing, which included fracture toughness and fatigue studies, was conducted to determine how wear correlated with better-understood mechanical behavior phenomena (e.g. plastic deformation). The metallographic analysis, which included automated quantitative metallography, was directed toward establishing quantitative, although perhaps empirical, relations between wear mechanisms and such microstructural parameters as second-phase size, size distribution, shape, orientation and hardness. The wear testing included characterization of the wear scar by computer-aided microtopographical examination, scanning and transmission electron microscopy and micro-quantitative analysis of phases.

1.2.2 Significant Results

Wear Testing

Low-stress abrasive testing in a rubber wheel abrasive test system (RWAT) with AFS 50-70 mesh silica abrasive (hardness KHN~1000) and similarly sized alumina abrasive (hardness KHN~2000) was conducted. Both fresh abrasives and those used in one previous test were employed to demonstrate the influence of abrasive breakdown on wear. Gouging wear tests were conducted in a test system (GAWT) in which the samples were pressed against alumina grinding wheels fabricated from the loose alumina used in the RWAT. Both tests were found to be highly reproducible with coefficients of variation within 4%.

Cast Irons

Tests throughout the program indicated that microstructure has a

marked effect on both low-stress and gouging wear resistance. For example, in pearlitic white irons, the higher the carbide volume fraction v_f, the greater the wear resistance. More surprisingly, carbide orientation was important, since wear resistance was lower perpendicular to than parallel to the carbide long axes.

Additional microstructural effects were evident in a series of Ni-hard 4 irons which consist of M_7C_3 carbides in a matrix of austenite decomposition product ($\alpha + Fe_3C$) with various amounts of retained austenite. RWAT test results with silica and alumina abrasive, GAWT test results against an alumina abrasive wheel and Amax pin tests (APT) indicated that, depending on the nature of the wear process, wear resistance may either be improved or decreased by the presence of retained austenite, so the potential for optimizing microstructure for specific wear applications was evident.

The studies on cast irons indicated that macrohardness was a good predictor of low-stress abrasion resistance, and a fair predictor of gouging wear resistance. Neither low-stress or gouging wear resistance correlated well to carbide microhardness, which susggested that the carbide-matrix interaction, rather than carbides alone, govern abrasive wear.

Mechanical property tests on the Ni-hard 4 irons indicated that wear correlated better to quasi-static tensile properties, such as compressive yield strength, than to measures of fatigue resistance or fracture toughness. These results underscore the role of carbide-matrix interactions during plastic deformation on abrasion. Scanning electron microscopy (SEM) studies coupled with energy dispersive X-ray spectroscopy (EDXS) clearly showed material attrition to occur by such conventional flow-fracture phenomena as matrix micromachining and carbide chipping and spalling. The relative importance of each material attrition phenomenon was greatly dependent upon applied load, abrasive hardness and abrasive angularity.

A manuscript based on the cast iron research was included in report COO-4246-8 and has been accepted for publication in Wear.

Co-base Alloys

The research indicated that the microstructures of the PM alloys have as strong an influence on abrasion resistance as do those of cast irons. In gouging applications and in low-stress applications against SiO_2, a moderately hard abrasive, wear resistance was a maximum for intermediate carbide v_f and alloy contents. Effort and expense required to increase matrix solid-solution strengthener content or carbide v_f beyond the maximum are actually counter-productive. In low-stress applications against Al_2O_3, a very hard abrasive, increasing alloy content monotonically increased wear resistance. As with the cast irons, the necessity of tailoring microstructure and composition to the specific wear application was evident.

For the Co-base alloys, Al_2O_3 RWAT wear resistance correlated moderately well to hardness, but SiO_2 RWAT resistance correlated in a less satisfactory manner. Wear scar microtopography gave a qualitative gauge of low-stress wear behavior in that the more resistant alloys had smoother wear scars. This suggests that uniform wear of matrix and carbide is desirable in these applications, and provides further evidence of the potential for improving wear resistance by microstructural control.

A manuscript summarizing research on the Co-base alloys is appended to this report and has been accepted for publication in the Proceedings of the 1979 AIME Symposium on Corrosion-Erosion Behavior of Materials

1.3 Objective and Scope of Phase II

1.3.1 Objectives

Since continuity of the research is desired between the two segments of the work, the five objectives of Phase II relate to the prior research and then extend into new materials and tests. The objectives are:

1. To refine the analysis of the wear, mechanical property and metallographic

data obtained in the first phase of the project on the alloy irons and Co-base alloys. The empirical relations previously developed will be put into forms which will couple wear to current theoretical expressions for flow-fracture material-attrition processes. This analysis may lead to a more basic understanding of wear and its relation to fundamental mechanical behavior.

2. To extend the testing and analysis program to a series of "balanced-composition" alloy irons of increasing carbide volume fraction and fixed matrix and carbide composition. These alloys contain sufficient alloying element to display good hardenability and high carbide hardness yet not so much that elements are wasted in causing excess retained austenite to be formed during processing. It is estimated that the market for such alloys, in coal crushing applications alone, is 3×10^{11} kg per year, with alloying element (particularly Cr) savings of $10^{7} - 10^{8}$ kg per year.
3. To extend the testing and analysis program to two series of Co-base PM alloys, one with lean matrix alloy content and one with rich matrix alloy content. Each series would contain samples with fine, medium and coarse carbide size. As with the alloy iron series, these alloys are commercially relevant, yet have microstructures which are systematically varied and amenable to a basic study of the mechanisms of abrasive wear.
4. To extend the program to two families of experimental alloys. The first are Ni-B PM alloys which may display comparable erosion and erosion-corrosion resistance to Co-base alloys at significantly lower cost. The second are ultrafine-carbide dispersion-strengthened PM alloys developed under the sponsorship of ARPA and which have potential for displaying exceptional mechanical properties.
5. To investigate the interrelation between abrasive properties (including degradation tendency) and wear in the RWAT and GAWT tests.

1.3.2 Scope

The five objectives in Phase II of the project are to be accomplished through the four tasks which comprise the Scope-of-Work. These tasks, and the sub-tasks involved in each of them are described below.

(Task I. Analysis of Co-base PM Data from Phase I)

1. Analyze existing RWAT and GAWT data in terms of QTM results, and establish quantitative empirical relations between wear behavior and quantitative metallographic parameters which define carbide size, shape and volume fraction.
2. Correlate existing RWAT and GAWT data to wear scar microtopography.
3. Conduct SEM studies of RWAT and GAWT data to wear scars in an effort to delineate flow-fracture processes governing material attrition.
4. Relate the empirical evidence generated in Task I, sub-tasks 1, 2 and 3, to fundamental theories of material, flow and fracture so as to elucidate the mechanisms of wear.

(Task II. Testing and Analysis of Balanced-Composition Irons)

1. Obtain a series of six as-cast specimens of a balanced-composition iron with systematically increasing carbide v_f and constant matrix and carbide composition.
2. Develop a range of microstructures in each sample by heat treatment and maximize RWAT and GAWT wear resistance. Heat treatments will consist of
   a) Austenitizing at 1040, 1095 and 1150°C (1900, 2000, 2100°F).
   b) Cooling at programmed rates already established at AMAX and ABEX laboratories to simulate thick-section heat treatments in practice .
   c) Stress relief-tempering at 200°C.

3. Characterize the microstructures developed by optical and quantitative metallographic techniques.
4. Determine RWAT and GAWT wear behavior of the various microstructural forms of the alloys.
5. Characterize wear scars by microtopography, SEM, and, if possible, TEM.
6. Obtain mechanical property data for the alloys in conjunction with AMAX laboratories.
7. Empirically correlate low-stress and gouging wear resistance to microstructure and mechanical properties, employing results of Task II, sub-tasks 1-6.
8. Attempt to develop quantitative relations between wear and mechanical behavior which elucidate the basic mechanisms of abrasion.

(Task III. Testing and Analysis of PM Alloys)

1. Procure the following series of PM alloys:
   a) Co-base alloys of moderate matrix solid-solution strengthener content (Alloy #6) with fine, medium and coarse carbide particle sizes.
   b) Co-base alloys of high matrix solid-solution strengthener content (Alloy #19) with fine, medium and coarse carbide particle sizes.
   c) Experimental Ni-B alloys.
   d) Experimental alloys with ultra fine carbide dispersion.
2. Conduct wear, microtopographic, QTM, SEM and if possible, TEM studies as in Task II, sub-tasks 2-5.
3. Develop empirical correlations as in Task II, sub-tasks 7 and 8.

(Task IV. Study of Abrasive-Target Interactions)

1. Characterize size distribution, shape, and hardness of loose fresh quartz and alumina abrasive to be used in RWAT testing.
2. Have fabricated abrasive wheels for the GAWT from the fresh quartz and alumina abrasive.
3. Characterize the size distribution, shape and hardness of spent quartz and aluminum abrasive after use in the RWAT and GAWT.
4. Employ spent quartz and alumina abrasive in additional RWAT tests.
5. Attempt to correlate differences in abrasiveness (fresh vs spent) to specific characteristics of the abrasives.
6. Procure silica sands in the AFS 50-70 size range having different angularity than the Ottawa silica so as to determine the influence of abrasive angularity on RWAT behavior.
7. Employ SEM to characterize the alloy wear debris from the above series of tests in order to determine how changes in abrasive properties influence material attrition mechanisms.

2. TASKS AND PROGRESS

2.1 Analysis of Co-base PM Data from Phase I

This task has been accomplished during the first three months of Phase II. The analysis is described in the manuscript appended to this report and accepted for publication in the Proceedings of the 1979 AIME Conference on Corrosion-Erosion Behavior of Materials

2.2 Testing and Analysis of Balanced-Composition Irons

The first sub-task in this task is procurement of a series of irons. Samples of 12 irons exhibiting a continuous increase in carbide v_f with constant matrix composition have been obtained from Climax Molybdenum Research Laboratories. The composition of the irons is given in Table I.

Optical and quantitative metallography (QTM) will be performed on these irons during the next quarter of the work.

2.3 Testing and Analysis of PM Alloys

The first sub-task of this task is the procurement of:

a) Three sets of PM samples of Co-base Alloy #6 (an alloy of moderate solid-solution strengthener content) with fine, medium and coarse carbide sizes.

b) Three sets of PM samples of Co-base Alloy #19 (an alloy of high solid-solution strengthener content) with fine, medium and coarse carbide sizes.

c) Experimental Ni-B alloys.

d) Ultra-fine particle size PM alloys.

The three sets of Alloy #6 and Alloy #19 have been obtained from Stellite Division, Cabot Corporation, Kokomo, IN. The chemical compositions are listed in Table II and the processing treatments used in generating the desired carbide sizes are presented in Table III.

Table I

CHEMICAL COMPOSITION OF THE HIGH CHROMIUM-MOLYBDENUM IRONS

(Climax Molybdenum Research Laboratories, Ann Arbor, MI, 48105)

Heat No.	Element, %								
	C	Si	Mn	Cr	Mo	Cu	Ni	P	S
6117A	1.41	0.58	1.56	11.6	2.39	1.24	0.020	0.018	0.030
6117B	1.38	0.58	1.56	12.8	2.39	1.24	0.020	0.018	0.030
6118A	2.00	0.59	1.54	15.8	2.35	1.14	0.020	NA	NA
6118B	1.89	0.59	1.54	17.8	2.35	1.14	0.020	NA	NA
6116A	2.58	0.56	1.50	17.6	2.39	1.03	0.023	0.020	0.030
6116B	2.48	0.56	1.50	18.7	2.39	1.03	0.023	0.020	0.030
6119A	2.87	0.58	1.52	20.0	2.36	0.94	0.020	NA	NA
6119B	2.79	0.58	1.52	21.0	2.36	0.94	0.020	NA	NA
6120A	3.50	0.61	1.59	23.4	2.47	0.87	0.022	0.020	0.030
6120B	3.41	0.61	1.59	24.1	2.47	0.87	0.022	0.020	0.030
6121A	3.93	0.60	1.57	24.6	2.45	0.76	0.022	NA	NA
6121B	3.81	0.63	1.57	25.7	2.45	0.76	0.022	NA	NA

NA = Not Analyzed

Table II

CHEMICAL COMPOSITION OF Co-BASE PM ALLOYS

(Stellite Division, Cabot Corporation, Kokomo, IN 46901)

Element	Alloy #6	Alloy #19
Co	Bal	Bal
Ni	1.16	2.00
Si	0.98	0.40
Fe	1.73	1.82
Mn	0.04	0.10
Cr	28.46	31.42
Mo	0.13	6.97
W	4.42	10.08
C	1.35	2.36
13	0.57	0.19

Table III

SINTERING TEMPERATURES FOR SPECIFIED CARBIDE SIZES

Alloy #6	Alloy #19
Set A - Fine Carbides - 1160°C	Set A - Fine Carbides - 1204°C
Set B - Medium Carbides - 1182°C	Set B - Medium Carbides - 1221°C
Set C - Coarse Carbides - 1204°C	Set C - Coarse Carbides - 1238°C

Alloy #6 : Stellite Heat 1063-76-020

Alloy #19 : Stellite Heat 1192-77-024

Optical and quantitative metallography will be performed on these alloys during the next quart of the work. In addition, plans will be made with Stellite for production of the Ni-B and ultra-fine PM samples.

2.4 Study of Abrasive - Target Interactions

No progress has been made on this task during the first quarter of Phase II.

3. SUMMARY

During this first quarter of Phase II of this project, effort has been con-concentrated on completion of Task I, Analysis of Co-base PM Data from Phase I. This task has been completed and the results are presented as a manuscript appended to this report. In addition, two of the four families of materials to be studied in Phase II, balanced - composition alloy cast irons and Co-base PM alloys, have been received. During the next quarter of the work these materials will be characterized and the remaining materials will be procured.

4. PERSONNEL

During this quarter of the research, the two co-investigators, Dr. Nicholas F. Fiore and Dr. Thomas Kosel, have devoted one-third time effort to the project. Three graduate Research Assistants joined the project at the end of the quarter and a Postdoctoral Fellow is scheduled to join it about December 1, 1979.

APPENDIX

MICROSTRUCTURE AND WEAR IN HIGH ALLOYS

by

T. H. Kosel, N. F. Fiore J. P. Coyle, S. P. Udvardy
and W. A. Konkel

(Accepted for publication in Proceedings of the 1979 AIME Symposium on Erosion - Corrosion -- Approved for publication by DOE)

MICROSTRUCTURE AND WEAR IN HIGH ALLOYS

T. H. Kosel, N. F. Fiore, J. P. Coyle, S. P. Udvardy, and W. A. Konkel
Department of Metallurgical Engineering and Materials Science
University of Notre Dame
Notre Dame, Indiana 46556

A series of Co-base powder metallurgy alloys has been tested for low-stress and gouging abrasion resistance. The test results have been examined with the objective of relating microstructural features to wear rates with the aid of scanning electron microscopy analysis of the worn surfaces.

Increasing the carbide volume fraction or alloy content of the materials to increase wear resistance is valuable to a point, but may actually be counterproductive beyond this point for some abrasion conditions. Macro-hardness is not found to be a reliable gauge of wear resistance for these alloys.

The response of the alloy carbides to different abrasives in low-stress abrasion depends on the angularity and hardness of the abrasive, and for softer abrasives carbide attrition controls the wear rate. The rigidly supported abrasive particles in the gouging abrasion test interact quite differently with the carbides than the same abrasive does in the low-stress test even under similar nominal loads.

Introduction

The effect of a second phase in an alloy on its abrasive wear behavior is expected to depend on the relative hardnesses of the two phases, the second phase volume fraction and particle size, and the strength of the interface between the two phases. The effects of such variables have been studied, but there is no general agreement as to the magnitude or even the direction of the effects, partly because the trends often reverse from one abrasion test to another (1). Some general trends, along with some of the conflicting observations, are cited below.

W. L. Silence (2), in a study of cast Co-base alloys, found that alloys with fine carbides produced in graphite molds wore 2.5 to 10 times faster than sand-cast alloys with coarse carbides. He concluded that in all cases studied, processing conditions generating coarser carbides resulted in lower wear rates for the SiO_2 abrasive rubber wheel test procedure employed. Dawson et al. (3) also found that wear rates increased as carbide size decreased. In contrast, Zum-Gahr (4) found that wear rates increased with carbide size for tool steels abraded in a pin test on SiC papers.

Increasing the volume fraction of a hard second phase should be expected to decrease wear rates, especially if the second phase is significantly harder than the abrasive. Larsen-Badse (5), in a study of carbon steels, found that wear rates decreased linearly as carbide volume fraction increased. However, the decrease was rather small, and the effect is probably due to the strengthening of the matrix by the carbides, since the carbides were much smaller than the width of the wear grooves. In another study (6), Larsen-Badse found that in S.A.P. alloys of Al_2O_3 particles in a matrix of Al, wear rates against SiC papers were lower for alloys with a larger volume fraction of Al_2O_3.

Alloys with large carbides, such as the Ni-hard 4 alloys studied by Fiore et al. (1), the alloys used by Silence (2), and those in the present study, gain wear resistance against SiO_2 abrasive from the resistance of the hard carbides (~1800 HK) to the softer abrasive (~900 HK). Fiore et al. (1) and Furillo (7) have shown that massive carbides protrude from the worn surface under low-stress abrasion with SiO_2. It was shown in the former study (1) that the carbides of Ni-hard 4 resist harder Al_2O_3 abrasive particles much less effectively than they resist SiO_2.

The present work is a study of the abrasion of a set of six commercially important Co-base powder metallurgy (PM) alloys tested against both SiO_2 and Al_2O_3 abrasives in a rubber wheel testing apparatus and in a gouging wear apparatus. In addition to the useful practical information obtained on the relative wear resistance of the alloys, the work allows some critical examination of possible material attrition micro-mechanisms which characterize the wear.

Experimental

The materials chosen for this study were six standard Stellite cobalt-base powder metallurgy alloys whose chemical compositions and densities are given in Table I and whose microstructures are shown in Figure 1. The alloys consist of an FCC Co-rich matrix containing solid solution strengthening elements and M_7C_3 and M_6C carbides. The M_7C_3 carbides have a hexagonal crystal structure and contain about 70 weight percent Cr, about 12 weight percent Co, and smaller amounts of the other metallic elements in the alloy. The M_6C carbides have a cubic crystal structure and are W rich; these occur only in the alloys 98M2, 3, and Star-J, which contain in excess of 10 weight percent W. Carbide sizes and volume fractions (V_f) were determined by standard quantitative metallographic techniques and are presented in Table II.

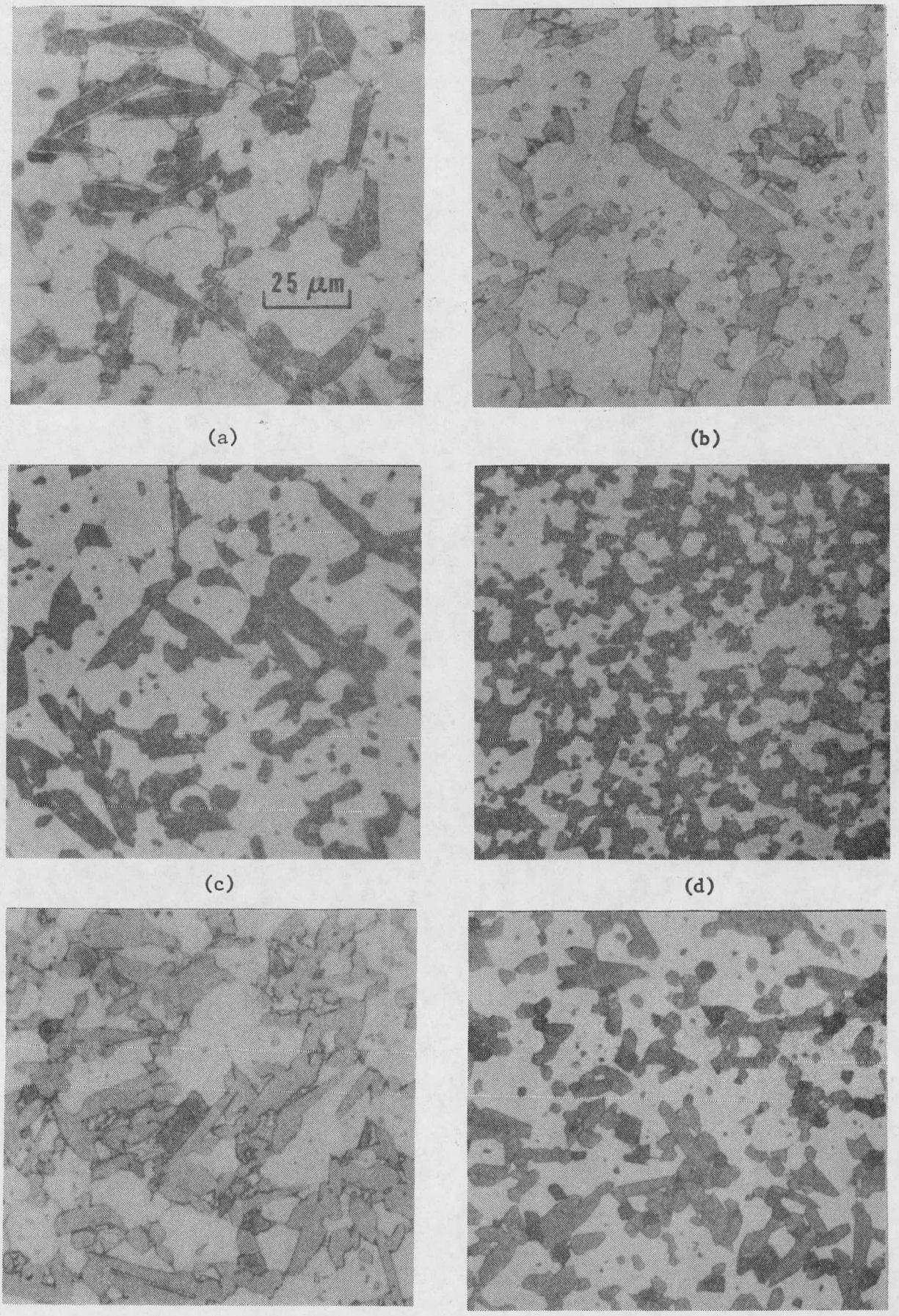

Figure 1. Microstructures of Co-base PM alloys. Magnifications are all the same as indicated in (a). (a) #6, (b) #6HC, (c) #19, (d) #98M2, (e) #3, (f) # Star-J.

Table I.

Chemical Compositions and Densities of Co-base PM Alloys

	#6	#6HC	#19	#98M2	#3	#Star-J
B	0.49	0.49	0.22	0.66	0.49	0.27
C	1.49	1.94	1.88	2.12	2.52	2.67
Co	Bal	Bal	Bal	Bal	Bal	Bal
Cr	28.99	28.99	30.17	30.57	30.91	31.57
Fe	1.46	1.46	1.92	3.09	2.29	0.32
Mo	0.32	0.32	--	0.24	0.35	0.02
Mn	0.13	0.13	0.65	0.23	<0.10	0.58
Ni	2.13	2.13	1.42	4.04	2.20	1.34
Si	0.92	0.92	--	0.51	0.51	0.34
V	--	--	--	3.82	--	<0.01
W	4.96	4.96	10.37	17.15	11.78	16.94
ρ (gm/cm^3)	8.38	8.38	8.54	8.63	8.64	8.76

Table II.

Carbide Sizes* and Volume Fractions†

	M_7C_3			M_6C			
Alloy	Length	Width	V_f	Length	Width	V_f	Total V_f
#6	27	6	33.8	--	--	0	33.8
#6HC	22	7	39.5	--	--	0	39.5
#19	26	7	37.4	--	--	0	37.4
#98M2	13	6	43.6	3	3	13.0	56.6
#3	29	9	46.3	10	7	8.9	55.2
#Star-J	21	6	41.0	8	6	8.9	49.9

*Carbide dimensions are in micrometers.

†Volume fractions are expressed as percentages.

Wear tests were conducted using two test machines described more fully in an earlier report (1). The first test is the rubber wheel abrasive test (RWAT), in which abrasive particles are fed between the specimen and a rotating rubber wheel. This test, designed to simulate low-stress abrasion, was conducted with 50/70 AFS test sand (SiO_2) and also with 50/70 Al_2O_3.

In the present work the weight loss after 3000 wheel revolutions was measured, whereas usually 1000 revolutions are employed. The abrasives were sieve-analyzed before and after testing, and because some degradation was discovered, further tests were made to determine the effects of this degradation on the abrasiveness of the particles.

The second test, the gouging abrasive wheel test (GAWT), simulates gouging abrasion conditions by using a bonded Al_2O_3 abrasive wheel. In both RWAT and GAWT tests, annealed 1020 steel is used as the control material.

The wear scars were examined in an ISI scanning electron microscope (SEM) interfaced to a Princeton Gamma-Tech energy dispersive x-ray spectroscopy system (EDXS). The EDXS capability allowed the identification of Cr-rich

carbides in the worn surface through the use of x-ray maps. Most SEM micrographs were taken using the secondary electron image mode, but in some cases enhanced contrast was obtained using back-scattered electron images.

Results

Wear Test Results

The RWAT weight losses for the SiO_2 abrasive are plotted versus R_c hardness in Figure 2a, and those for Al_2O_3 are displayed in Figure 2b. The GAWT abrasion factors (specimen weight loss divided by the weight loss of 1020 steel standards) are plotted against R_c hardness in Figure 2c. The RWAT results include data obtained with abrasive previously used in another test, as will be discussed later. Each point shown is the average of three tests. The error bars for the SiO_2 RWAT test would be about ± 0.005 grams (~6%); those for the Al_2O_3 would be about ± 0.1 grams (~5%); and those for the GAWT would be about ± 10%. If the wear rates were inversely proportional to hardness, the points would lie on hyperbolas. The lack of a clear correlation between wear and R_c for the SiO_2 RWAT and the GAWT results is apparent, although wear correlates with R_c hardness much more closely in the Al_2O_3 RWAT test.

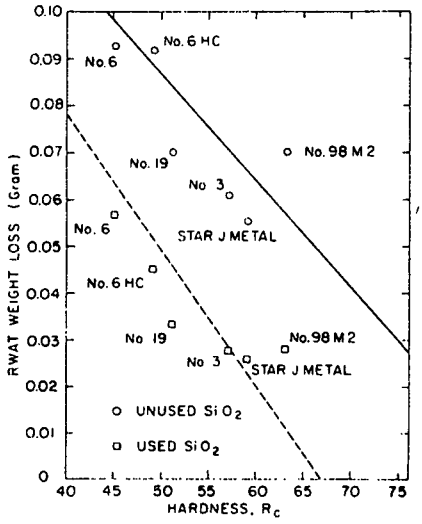

(a)

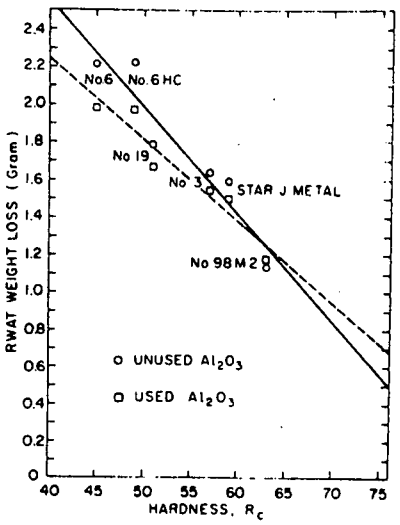

(b)

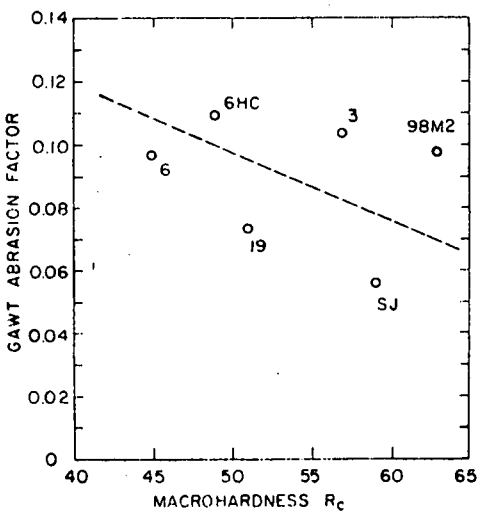

(c)

Figure 2. Wear test results plotted versus R_c hardness.
(a) Unused and used SiO_2 RWAT,
(b) Unused and used Al_2O_3 RWAT,
(c) GAWT.

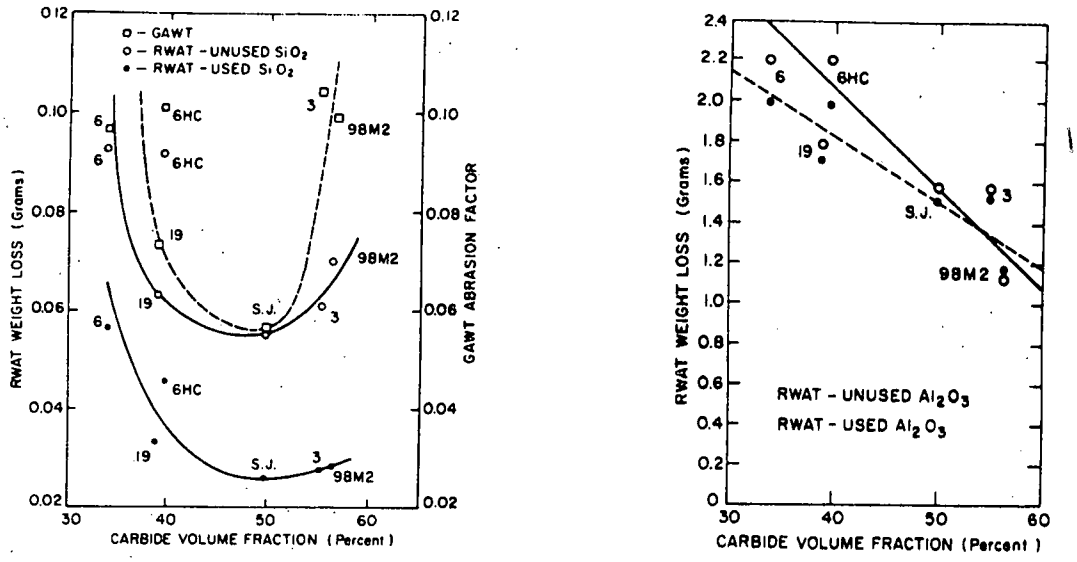

(a) (b)

Figure 3. Wear test results plotted versus carbide volume fraction. (a) SiO_2 RWAT and GAWT, (b) Al_2O_3 RWAT.

One parameter which might be expected to affect wear rate is the carbide volume fraction, V_f. Plots of wear versus V_f are shown in Figure 3. The Star-J alloy shows the lowest weight loss for both the SiO_2 RWAT test and the GAWT test. As V_f increases beyond the value for Star-J, the wear rate increases again for these two tests. This is not the case in the Al_2O_3 RWAT test, in which the wear rate decreases monotonically with V_f.

Another parameter which might be expected to affect wear rates is the matrix strength. Since this is not known accurately for these alloys, normalized alloy content was taken to be a measure of matrix strength. This was defined as the sum of the weight percentages of Ni, V, and W in the alloys, normalized against alloy #6. The values for the alloys are shown in Table III together with the Rockwell C (R_C) hardness values. Normalized alloy content gives an approximate measure of the solid solution strengthening of the matrix, as will be discussed in more detail later. As is seen from Figure 4, the wear rates follow trends with normalized alloy content similar to those with V_f. The SiO_2 RWAT and GAWT weight losses pass through minima at the Star-J alloy, whereas wear rates decrease monotonically with both V_f and normalized alloy content for the Al_2O_3 RWAT test.

Table III.

Normalized Alloy Content and R_C Hardness of PM Alloys

Alloy	#6	#19	#6HC	#Star-J	#3	#98M2
Hardness (R_C)	45.0	51.0	49.0	59.0	57.0	63.0
Normalized Alloy Content	1.0	1.7	1.0	2.6	2.0	3.5

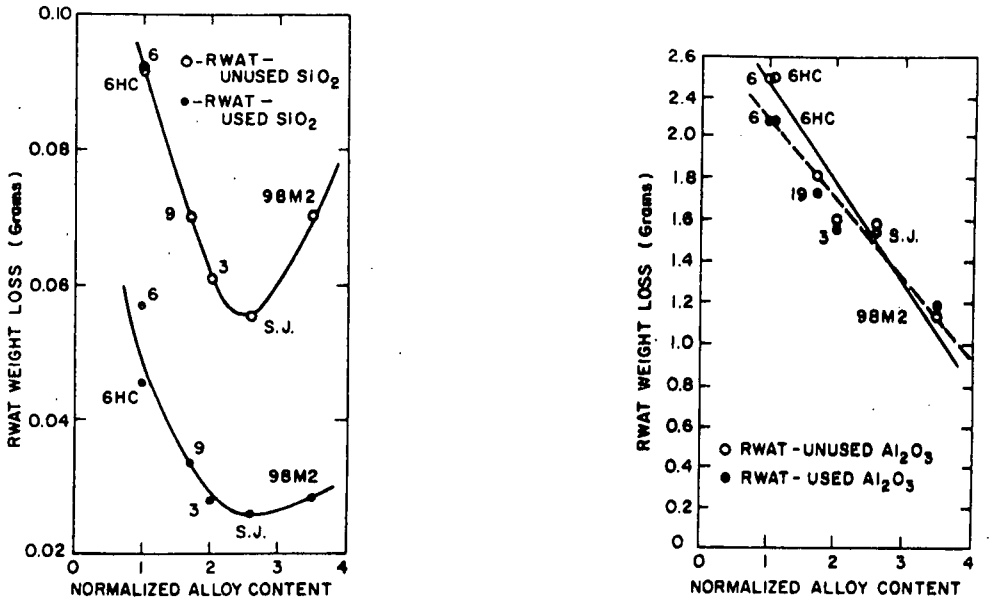

Figure 4. Wear test results plotted versus normalized alloy content. (a) SiO_2 RWAT, (b) Al_2O_3 RWAT.

Abrasive Degradation

The results of the sieve analysis of the SiO_2 and Al_2O_3 RWAT abrasives before and after use in wear testing are shown in Figures 5a and 5b. The SiO_2 abrasive breaks down after one test, so that a considerable increase in the number of particles in the finer sizes is observed. A second test further increases the number of finer particles. The Al_2O_3 abrasive also breaks down after the first test, but does not break down measurably in response to a second test. SEM micrographs of the SiO_2 and Al_2O_3 abrasives are shown in Figure 6. (The used abrasives are practically indistinguishable

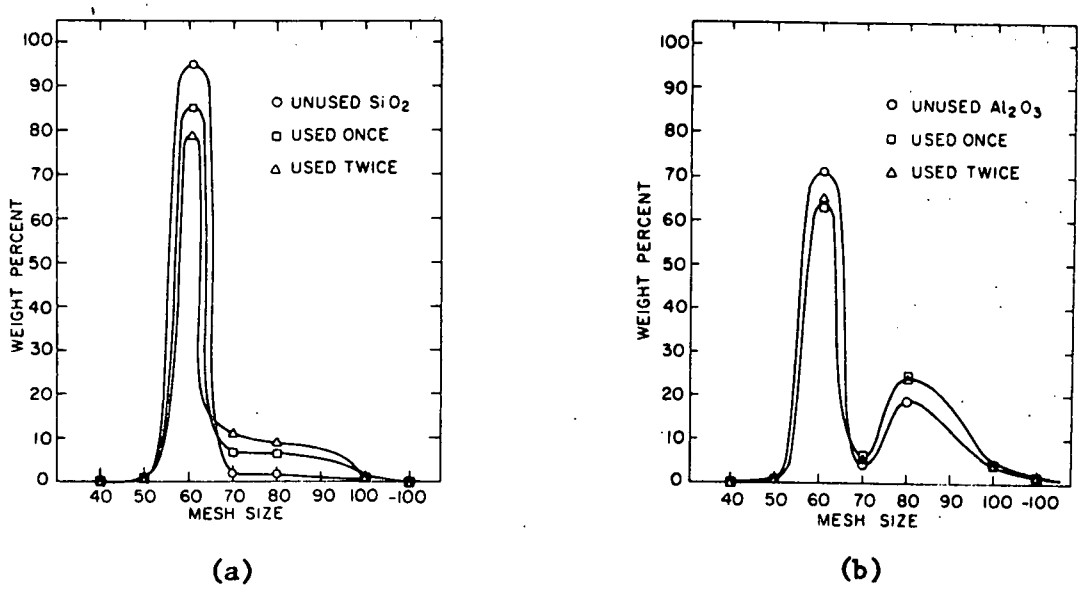

Figure 5. Sieve analysis results of RWAT abrasives before and after use against Co-base alloys. (a) SiO_2, (b) Al_2O_3.

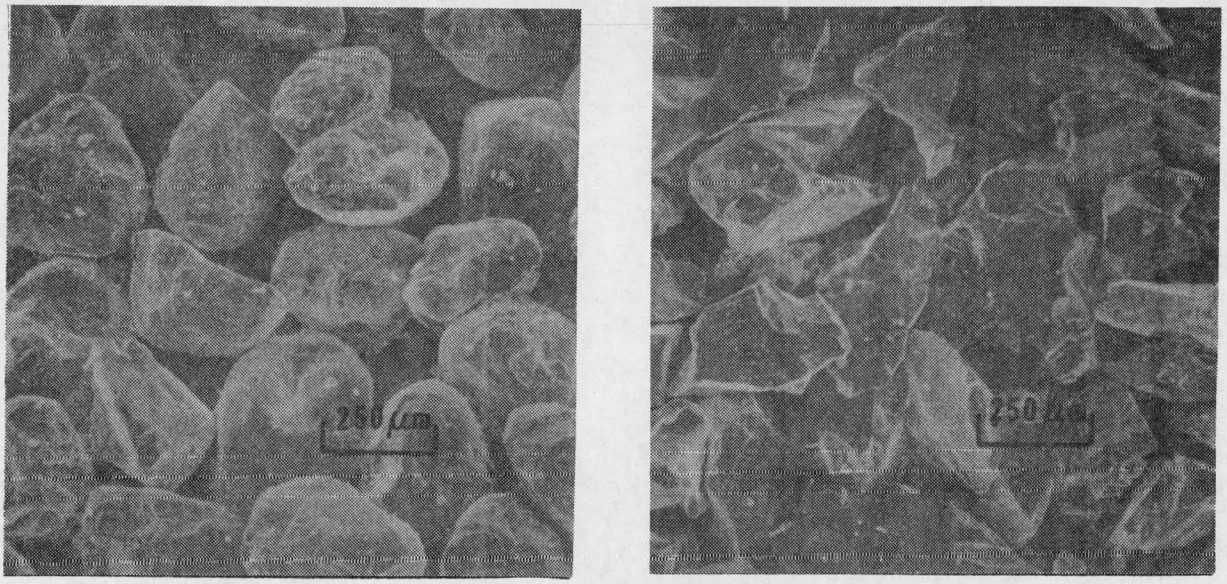

(a) (b)

Figure 6. Typical SEM micrographs of RWAT abrasives. (a) SiO_2, (b) Al_2O_3.

from the new in the SEM.) The Al_2O_3 particles are considerably more angular than the SiO_2, and in addition they are much harder (~2000 HK) than the SiO_2 abrasive (~900 HK). However, changes in the angularity of the particles as a result of testing are very difficult to detect because the unused and degraded particles are so similar in appearance.

The wear test results in Figure 3a indicate that the SiO_2 loses approximately 50% of its abrasiveness after one test for the Stellite alloys. However, steel specimens showed that the used abrasive did not give measurably lower wear rates for this material. For the Al_2O_3, abrasive breakdown caused only a minor decrease in weight loss of the Co-base alloys (Figure 3b) and only about a 10% decrease in weight loss of the 1020 steel standards.

The new Al_2O_3 abrasive produced weight losses which averaged 25 times as large as those for the new SiO_2 in the RWAT. In contrast, the 1020 standard specimens wore 4 times as fast with new Al_2O_3 as with new SiO_2.

SEM Observations

SEM micrographs of the RWAT wear scars caused by new SiO_2 are shown in Figures 7, 8, and 9 for alloys #6, Star-J, and 98M2. These figures include examples of the x-ray maps used to identify the Cr-rich M_7C_3 carbides and the W-rich M_6C carbides. In the #6 alloy (Figure 7), the large M_7C_3 carbides protrude markedly from the surface, and the matrix is worn preferentially. Deep grooves in the matrix often end at one side of carbide particles and reappear at the other side, indicating that the SiO_2 abrasive particles are unable to cut the hard carbides. Preferential wear of the matrix is also apparent in the Star-J alloy (Figure 8) and in alloy 98M2 (Figure 9). Star-J and 98M2 both contain W-rich M_6C carbides, which exhibit a characteristic light contrast in the SEM, as shown by comparison of the W x-ray map of Figure 8d with the corresponding secondary electron image in Figure 8b. The M_7C_3 carbides in alloy Star-J tend to appear slightly darker than the matrix (Figure 8), whereas in alloy 98M2 they generally appear somewhat lighter than the matrix.

(a)

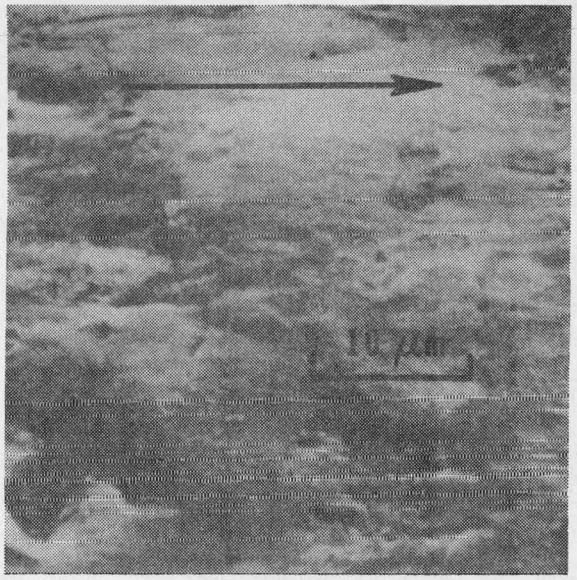

(b)

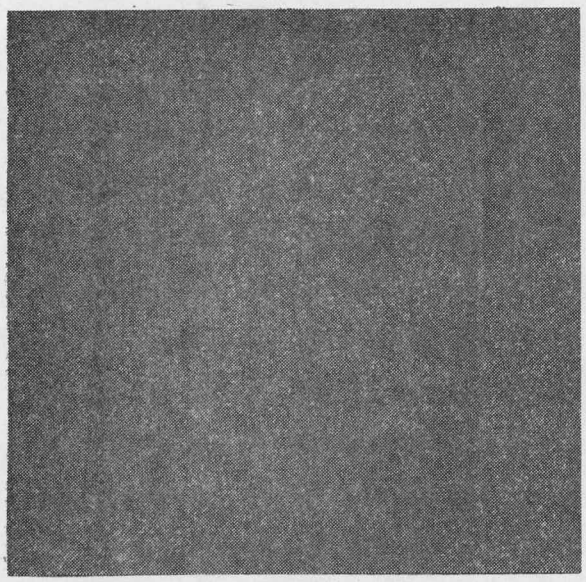

(c)

Figure 7. SEM micrographs of SiO_2 RWAT wear scar in alloy #6. (a) Low magnification, (b) Higher magnification area showing wear debris at A, (c) Cr x-ray map of (b). Direction of abrasive flow indicated by an arrow here and in later RWAT micrographs.

Some interesting yet not understood observations relate to RWAT wear debris on the scar surfaces. In alloy #6 there is evidence that the debris is piled up against those carbides whose leading edges make large angles with the direction of abrasive flow; for example, at A in Figure 7b. Such areas are also identifiable by optical metallography, with the debris appearing darker than the matrix, and often extending in front of the carbide for a distance comparable to the width of the carbide. In the SEM, the debris areas have a much rougher appearance than other matrix areas (Figure 7b). In alloy #6 the raised areas associated with carbides are often much larger than the carbides themselves due to the presence of a mass of debris at the leading edge and a tapered area of grooved matrix material at the trailing edge (Figure 7b). In alloy Star-J, the raised carbides do not have such large areas of raised matrix material associated with them.

The marked difference in M_6C and M_7C_3 sizes is evident for the 98M2 alloy, and the smaller M_6C carbides in this material appear to be pulled from the matrix by the SiO_2 abrasive (Figure 9). These small carbides may contri-

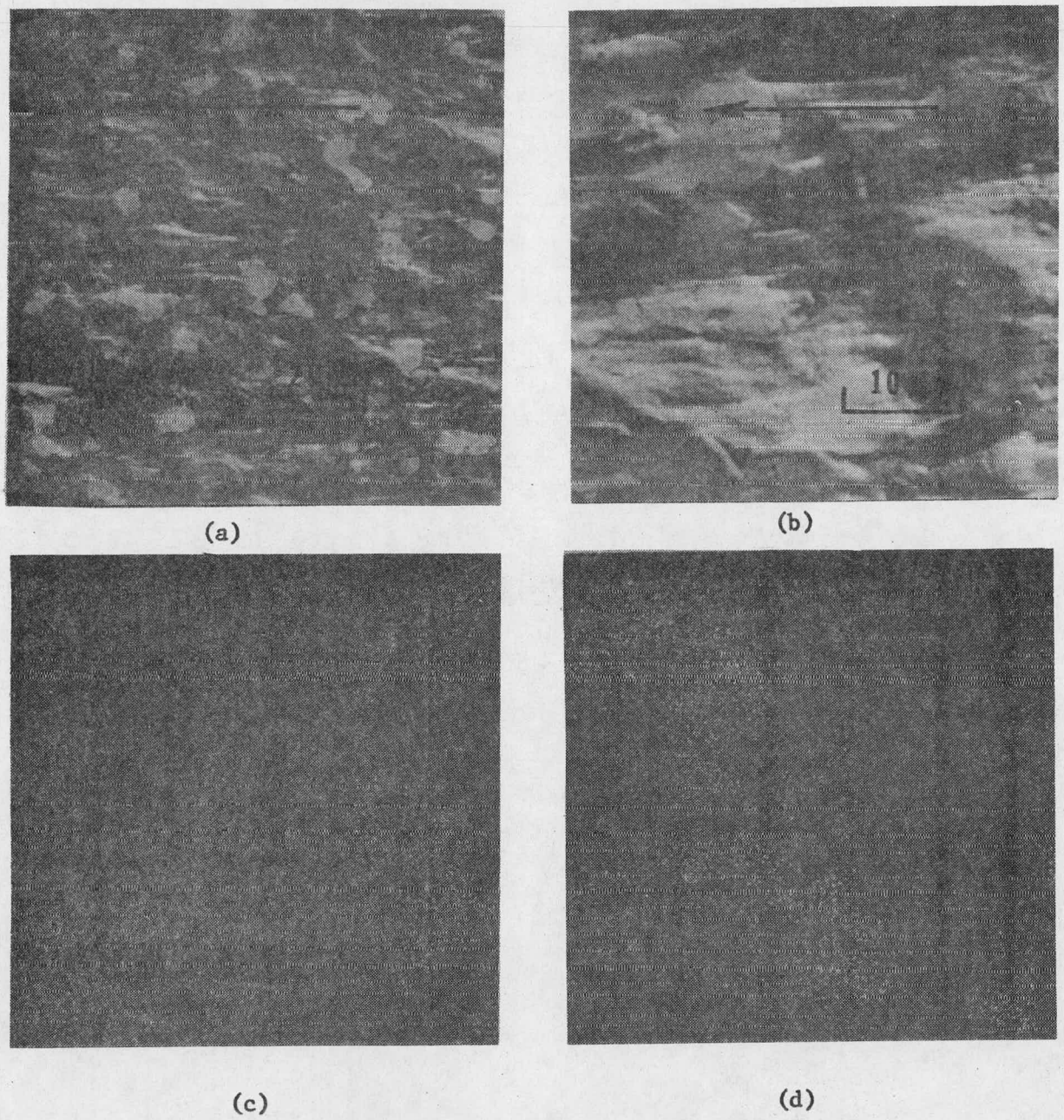

Figure 8. SEM micrographs of SiO_2 RWAT wear scar in alloy Star-J. (a) Low magnification, (b) Higher magnification, (c) Cr x-ray map of (b), (d) W x-ray map of (b).

bute to the abrasion, because in some cases distinct grooves of the same size as the small carbides are found in the larger carbides.

SEM micrographs of the #3 alloy, not shown here, were very similar to those from the Star-J alloy.

SEM micrographs of the Al_2O_3 RWAT wear scars are shown in Figure 10. It is apparent that this harder abrasive is able to effectively cut the alloy carbides, but the carbides still protrude from the surface to some extent, indicating preferential removal of the matrix. This is more apparent in micrographs taken with the direction of abrasive flow from top to bottom than in those with flow from left to right due to a contrast effect in the SEM, as shown by the comparison of Figures 10a and 10b. The detector in the SEM

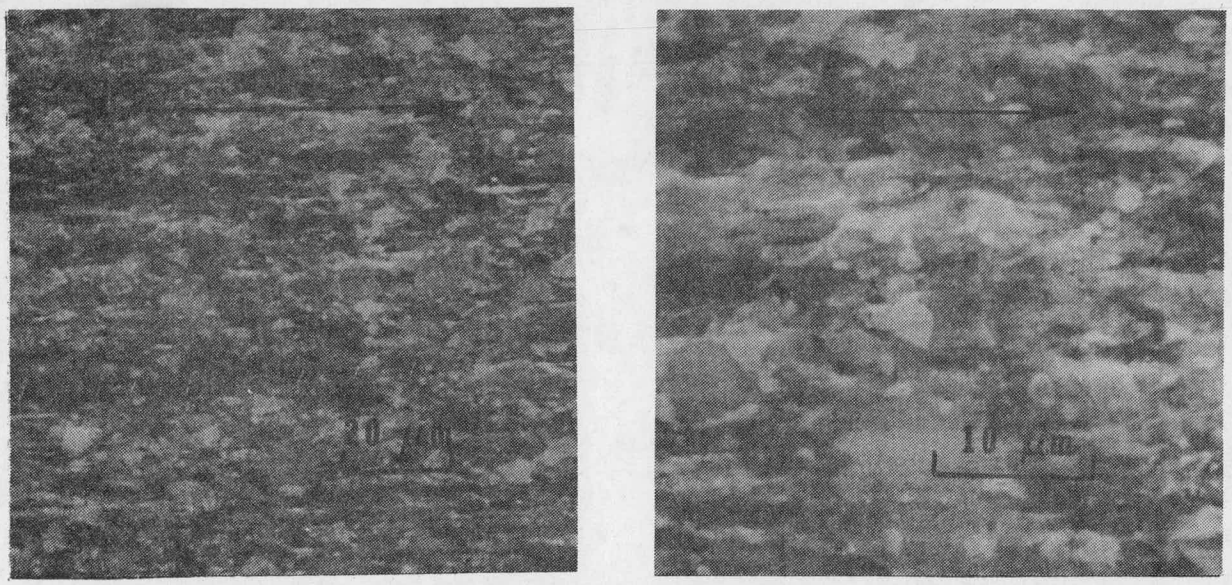

(a) (b)

Figure 9. SEM micrographs of SiO_2 RWAT wear scar in alloy 98M2. (a) Low magnification, (b) Higher magnification. M_6C carbides appear white, M_6C appears smooth, and the matrix areas are heavily gouged and darker than the M_7C_3.

corresponds to the apparent source of light, and this is fixed at the upper right corner of the picture for these micrographs. Because the leading and trailing edges of the carbides are more steeply inclined to the surface than are the sides, the shadowing of carbides is more pronounced in micrographs with the flow from top to bottom. Careful examination of several micrographs shows that in many instances the deep grooves in the matrix become narrower when the abrasive particle enters a carbide, again indicating that the carbides resist the abrasive more effectively than the matrix (e. g., Figure 10b). It is interesting to note that because of the shadowing effect mentioned above, carbides appear to be depressed rather than raised when the micrographs are viewed upside down.

SEM micrographs of the GAWT wear scars of alloys #6, Star-J, 3, and 98M2 are shown in Figure 11. The grooves cut by abrasive particles are much deeper than in the RWAT with either abrasive. In alloy #6, large pits are frequently observed, and these are identified with the aid of Cr x-ray maps as sites of fractured, partially removed carbides in nearly all cases (Figure 12). In a few cases such pits did not seem to be Cr-rich (which would indicate the presence of M_7C_3), but since such pits had smoother surfaces inside, they were interpreted as being sites where smaller carbides had been pulled out completely. Many carbides appeared to be slightly fractured and partially covered with smeared metal.

The appearance of the Star-J GAWT wear scar is similar to that of alloy #6, except for the presence of the light-colored M_6C carbides. Pits associated with fractured carbides are also observed in Star-J. The GAWT wear scar of alloy 98M2 shows a roughness in the grooves of a size scale comparable to that of the smaller M_6C carbides in this material (about one or two microns), suggesting that this roughness is caused by direct removal of the small carbides. Many small pits one or two microns across, which correspond to the size of the smaller M_6C carbides, are observed. There are also gaps adjacent to many small carbides which may be sites where the matrix has been pulled

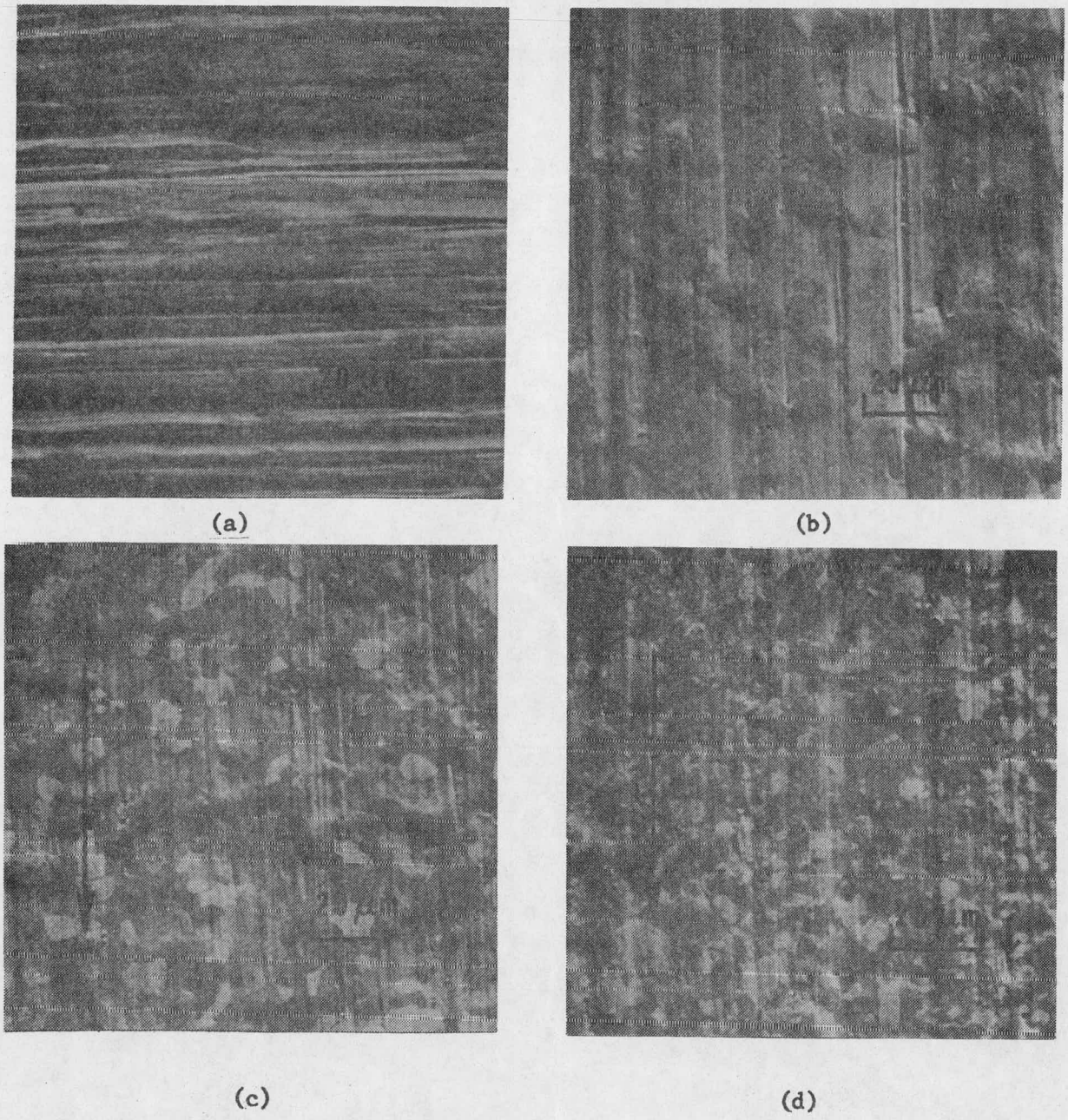

Figure 10. Al_2O_3 RWAT wear scars. Directions of abrasive flow are indicated. (a) Alloy #6, (b) #6, (c) #Star-J, (d) #98M2.

away from the carbides, making their subsequent removal easier. In addition, the edges of the grooves in 98M2 often have a serrated appearance where small carbides probably have been torn loose from the thin ribbon of material formed at the side.

Alloy #3 shows a GAWT wear scar which is very similar to that of the Star-J alloy, despite the fact that the wear rate of alloy #3 was nearly twice as high.

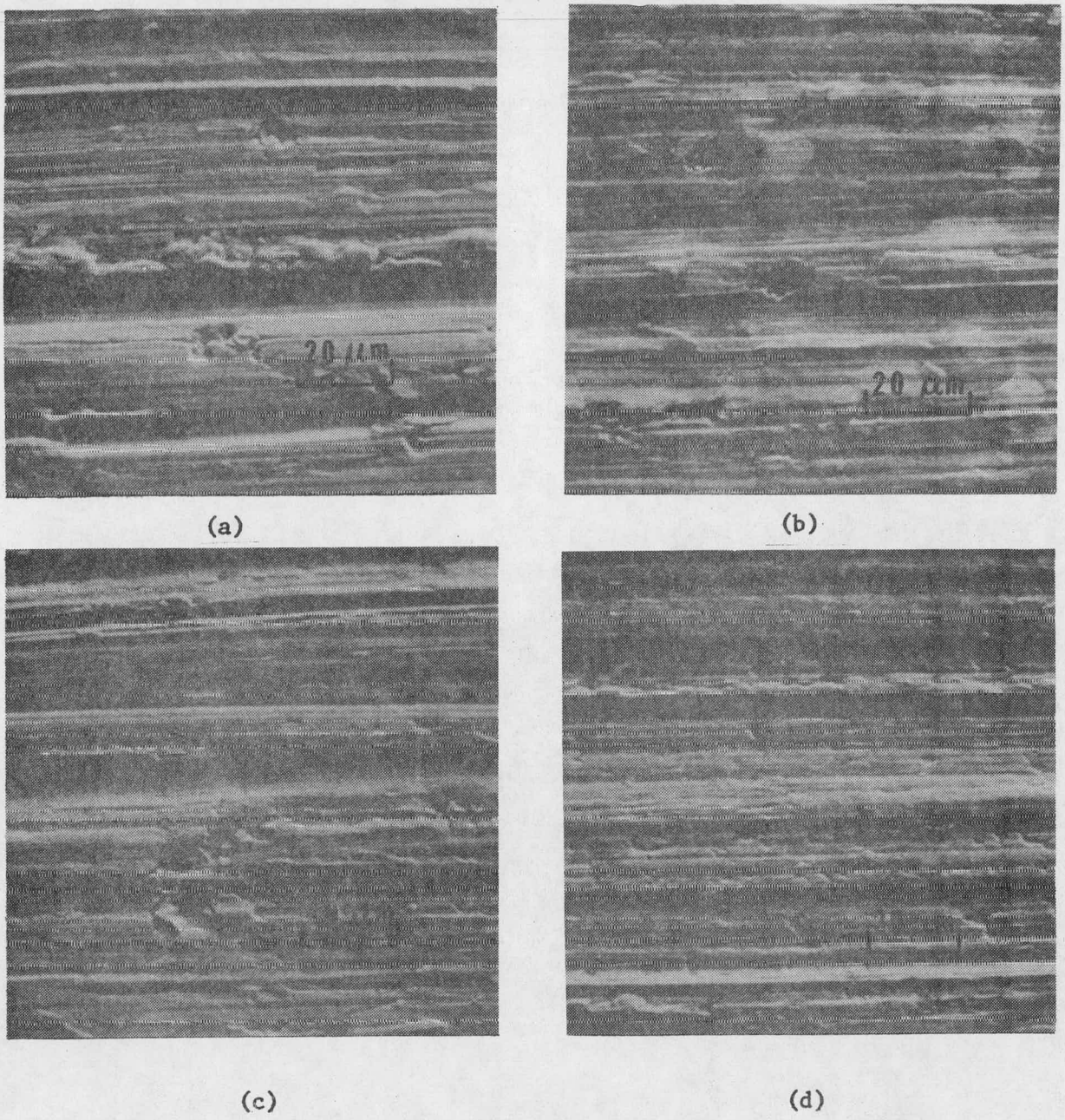

Figure 11. GAWT wear scars. (a) Alloy #6, (b) #Star-J, (c) #3, (d) #98M2.

Discussion

General Discussion of Wear Test Results

In the SiO_2 RWAT and GAWT tests a minimum wear rate occurs at an intermediate value of either V_f or normalized alloy content (Figures 3 and 4). Alloying to provide increased wear resistance is thus counterproductive beyond a certain point for service conditions corresponding to these two tests. However, for the Al_2O_3 RWAT test, the wear rate continues to decrease as V_f and normalized alloy content increase. Thus the choice of an alloy for optimum wear resistance appears to depend on the service conditions to be encountered. Possible reasons for this will be discussed later.

The normalized alloy content parameter is used here to give a measure of matrix strength because reliable microhardness values are not available, due

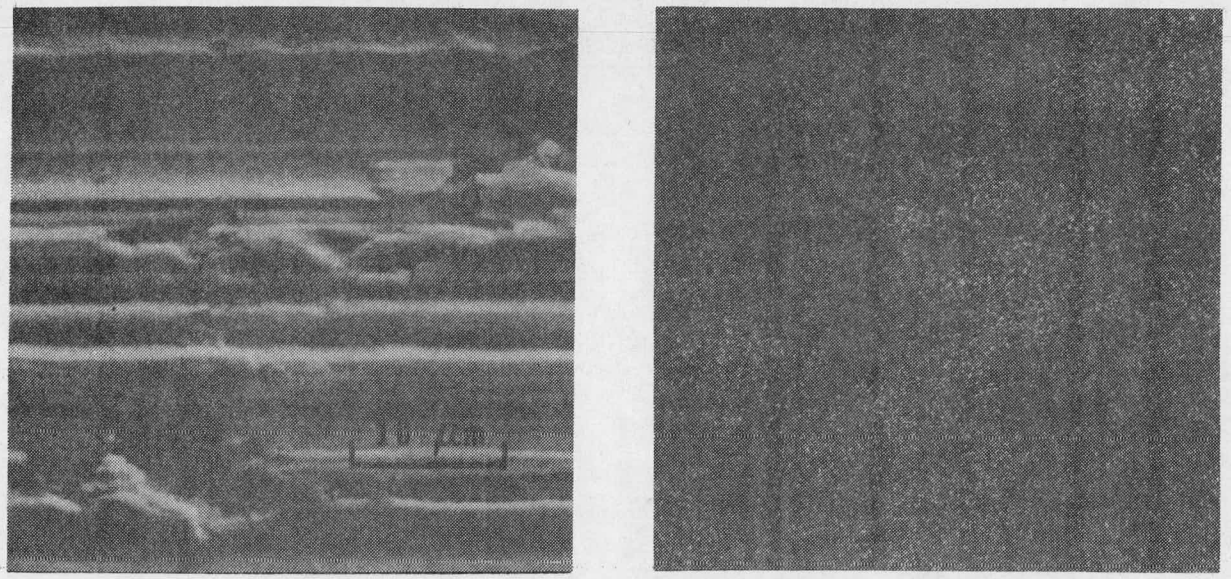

(a) (b)

Figure 12. Identification of fractured Cr-rich M_7C_3 carbide in GAWT wear scar of alloy #6. (a) SEM image, (b) Cr x-ray map.

to the difficulties associated with measuring microhardness in the very small matrix areas between carbides. Although a quantitative measure of matrix alloy content would have to take into account the partitioning of alloying elements between carbides and matrix (2), the normalized alloy content used here gives at least a qualitative measure of matrix strength.

RWAT Tests

Macrohardness is the most commonly used indicator of probable wear resistance, but it is found to be unsatisfactory in this study, except possibly for the Al_2O_3 RWAT results. The simple theory of abrasive wear (8) is based on the concept of an abrasive particle which forms a groove whose depth varies directly with applied load and inversely with the macrohardness of the material. All of the material in this groove is assumed to be removed in a single cutting event. The limitations of the latter assumption are discussed clearly by Murray, Mutton, and Watson (9). Depending on the rake angle of the abrading particle and on the material, cutting interactions may occur with chip formation, or ploughing interactions may simply plastically displace material. Since this effect is neglected in the simple theory, it is not surprising that the theory is unsatisfactory.

Even if the simple model of abrasion were modified to take into account rake angle, it would not adequately describe the present case of two-phase alloys in which abrading particles alternately encounter areas of relatively soft matrix and hard carbides. In such cases the simple theory must at least be modified to include some sort of averaging of the wear rates of the two phases.

This averaging will in many cases not be as simple as correcting for the area fractions of the phases, because under some conditions the slowest wearing phase will control wear. For instance, in the present study the SiO_2 RWAT data do not fit the prediction that wear is inversely proportional to hardness, and the SEM results clearly show that the matrix phase is preferentially removed. As discussed by Fiore et al. (1), under these conditions the removal of the hard carbide phase is controlling, because removal of the

matrix material between the carbides is prevented by the fact that the large abrasive particles usually touch two adjacent carbides. The carbide sizes and inter-carbide spacings in these materials are about 30 microns, whereas the rounded SiO_2 abrasive particles are about 250 microns in diameter. Thus the rate at which the matrix phase is removed is determined by the removal rate of the adjacent carbides.

There is evidence as to the manner of carbide attrition, the process which controls wear in these tests. In previous work (1) on Ni-hard 4 cast irons, large carbides were observed to be preferentially grooved on the leading edges during SiO_2 RWAT testing, and it was concluded that the carbides were gradually removed by attrition of the edges. In the present work, this is probably also the case. Since gross carbide fracture in the SiO_2 RWAT is seldom observed, the carbides probably are removed gradually by fine-scale chipping or cutting events. Under such conditions one would expect alloys with higher V_f to have lower wear rates, all other things being equal. This simple behavior is not observed (Figure 3). However, as V_f increases, the macrohardness, the matrix phase hardness, carbide size, and possibly carbide hardness vary as well. The increase in wear rate with V_f after the minimum is probably due to the interaction of these variables. The SEM observations suggest that the reason that the 98M2 alloy, which has both the highest V_f and macrohardness, has less abrasion resistance than expected is that many of the very small M_6C carbides are pulled out of the matrix. The carbides thus contribute to V_f but not to the wear resistance, and to some extent they also increase the wear rate by becoming abrasive particles themselves.

The contribution of the pulled-out carbides should be rather small since the carbides would comprise a small fraction of the abrasive material. Also, soon after being pulled out they probably would be carried along between the large abrasive particles. Regardless of the relative magnitudes of the losses of wear resistance due to pull-out and to subsequent abrasiveness of the small carbides, the probable reason for the relatively poor abrasion resistance of 98M2 against SiO_2 is carbide removal.

In both the Al_2O_3 and the SiO_2 RWAT tests, the matrix is preferentially worn, leaving carbides standing in relief. With Al_2O_3, however, this effect is much less pronounced than for the SiO_2 abrasive, since the carbide relief is seen only in micrographs taken with the abrasive flow from top to bottom. This is understandable, since the Al_2O_3 is comparable in hardness (~2000 HK) to the M_6C carbides (~1800 HK), while the SiO_2 is substantially softer (~900 HK) than the carbides.

Carbide V_f would not be expected to be the sole controlling factor in Al_2O_3 tests because the carbides are being cut effectively by the abrasive particles. The matrix is therefore less protected by them. In addition, the more angular Al_2O_3 particles would probably penetrate into the matrix phase between carbides more effectively than the rounded SiO_2 particles. Since the carbide V_f probably plays a smaller role here than for SiO_2, a change in alloy ranking is not surprising. The SEM results suggest that higher V_f should increase wear resistance here since the carbides resist penetration, and matrix strength should also play a part since the matrix wear rate is comparable to that of the carbides. Since both of these increase macrohardness, a monotonic decrease in wear with R_c is observed.

GAWT Tests

Even though the nominal load between specimen and wheel is lower for the GAWT (0.127 MPa) than for the RWAT (~0.4 MPa), it is observed that the Al_2O_3 particles penetrate the carbides more effectively in the GAWT. This is probably due to the fact that the abrasive particles in the GAWT wheel are

rigidly supported, giving rise to different particle loading conditions when hard carbides are encountered. The particles in the RWAT test form approximately a close-packed monolayer between specimen and wheel, and the average load per particle is the total load divided by the number of particles. However, when an individual abrasive particle encounters a hard carbide in the RWAT test, it can be deflected into the wheel, increasing its load only slightly. In the GAWT test, when an abrasive particle encountering a large carbide begins to deflect over it, the other particles of the wheel must also deflect simultaneously. Their loads are thus decreased, and the load on the particle encountering the carbide is increased very rapidly as the deflection begins. The cutting force on the particle thus becomes sufficient to penetrate the carbide before a large deflection of the wheel occurs. The abrasive particle may fracture or the carbide may be fractured, cut, or ploughed (9,10), depending on the rake angle. In contrast, the RWAT particles are relatively easily deflected by carbides. It is not surprising in view of this difference in particle loading characteristics that alloy rankings often change between RWAT and GAWT tests (1).

The SEM observations indicate that the small M_6C carbides in the 98M2 alloy tend to be pulled out in the GAWT test, but this cannot be the case for alloy #3, which has larger carbides. The SEM observations do not show a significant difference in the wear scars of the alloys #6, Star-J, and #3, and although it is tempting to ascribe the upswing in the wear rate versus V_f curve to pull-out of small carbides as in 98M2, this is not borne out in alloy #3.

Abrasive Degradation

The RWAT test was designed to simulate low-stress abrasion conditions, in which it is assumed that the abrasive is unaffected by the test. That this is not the case is evident from the sieve analysis results on the used abrasives. This observation may have implications regarding the reproducibility of RWAT results with different batches of the "same" abrasive, since small changes in the abrasive are apparently capable of producing rather large changes in its abrasiveness.

The abrasiveness of SiO_2 is reduced by about half against the Co-base alloys, but does not decrease against 1020 steel. This is difficult to understand, since changes in abrasive size or shape would be expected to affect the response of different alloys in similar ways, if not quite to the same extent. Larsen-Badse (11,12) has examined the effect of abrasive particle size on wear rates and determined that above a critical grit size, wear rate tends to become independent of abrasive size. This suggests that the observed size reduction of the abrasive should not lead to substantial changes in wear rate since the abrasive used here is large compared to the size at which wear rates become insensitive to particle size. However, Larsen-Badse's studies (11,12) were conducted with SiC abrasive papers, and the dependence of wear rate on particle size may differ for the rubber wheel test of the present study.

The change in abrasiveness of the Al_2O_3 was rather small against all materials. The sieve analysis results characterize size changes, but shape changes (rounding, etc.) are much more difficult to define. Since long continuous grooves are produced on the specimens, abrasive particles must contact specimens at just one point or edge, so that most of the particle would not be blunted or affected. (As noted earlier, the size of the grooves is much smaller than the size of the particles.) Since loose abrasives are employed in the RWAT, the corner of the particle which actually contacted the specimen is unknown, and so it is not possible to determine whether a particular corner under observation has undergone degradation. The fact that only

one edge or point of a particle is affected by a given test probably means that significant rounding of the particles requires many abrasion events, so it seems likely that the observed decreases in abrasiveness of the particles are primarily due to the size change.

Effects of Abrasive Type

The fact that the Co-base alloys wore about 25 times faster against new Al_2O_3 than against SiO_2 abrasive in the RWAT can be ascribed to the combined effects of the greater hardness and angularity of the Al_2O_3 particles. The 1020 standard specimens consisting of ferrite plus pearlite wore only about four times faster using Al_2O_3. The thin Fe_3C platelets of the pearlite would not be expected to resist even the softer SiO_2 abrasive very effectively, and the increased angularity of the Al_2O_3 is probably primarily responsible for its increased abrasiveness against 1020 steel.

This suggestion is in agreement with results reported by Avery (13), who found an increase by a factor of 3.7 in the wear rate of 1020 steel for angular Wausaw crushed SiO_2 compared to rounded Ottawa SiO_2 of the same grit size, using a rubber wheel abrasion test. Preliminary results of Swanson (14) also indicate that crushed quartz is four times as aggressive against 1020 steel as the rounded AFS test sand normally used in the RWAT.

The hardness of the Al_2O_3 particles provides an additional increase in abrasiveness against the Co-base alloys due to their ability to penetrate the large carbides. It is also interesting to note that the 98M2 alloy wore only 16 times faster against Al_2O_3, while all the other Co-base alloys wore between 24 and 30 times as fast. This is consistent with the argument that increased abrasive hardness increases wear rates more for alloys with larger carbides.

Conclusions

1. Alloying Co-base PM alloys to provide increased carbide V_f or matrix strength improves abrasive wear resistance in low-stress wear against hard abrasives. Against softer abrasives or in gouging conditions it is valuable to a point, but may actually be counterproductive beyond this point. The abrasion behavior of a given microstructure is a strong function of the specific abrasion conditions, and the use of broad generalities in predicting wear resistance is not warranted.

2. For these alloys, macrohardness is a satisfactory gauge of wear resistance in low-stress applications against very hard abrasives. It is unsatisfactory in low-stress applications against softer abrasives or in gouging applications.

3. The simple inverse-hardness description of abrasive wear must be modified to take into account the rake angles of abrading particles, the size and hardness of multiphase particles, and the matrix-particle interactions.

4. Closely spaced large carbides protect the matrix against wear under low-stress abrasion conditions, and carbide attrition rather than matrix attrition governs wear rates.

5. Small second-phase particles may be dislodged from the matrix during wear, resulting in marked weight losses and actually enhancing the abrasion environment.

6. The load-time history on an abrasive particle in gouging wear has a strong influence on material attrition. The same abrasive employed under

low-stress and gouging conditions acts quite differently in the two applications, even under similar nominal loads.

7. One of the most commonly accepted low-stress abrasion tests causes degradation of the abrasive. This degradation usually decreases the effectiveness of the abrasive.

8. In low-stress abrasion against materials with large carbides, hardness and angularity of the abrasive control wear. Against alloys with small carbides, angularity appears to be more important than hardness.

Acknowledgments

This work has been supported by the Division of Fossil Energy, U.S. Department of Energy; the authors are indebted to the staff for their cooperation. They also thank Dr. R. Grierson and K. Antony, Stellite Division, Cabot Corporation, for providing the alloys and commentary on the experimental program.

References

1. N. F. Fiore, J. P. Coyle, S. P. Udvardy, T. H. Kosel, and W. A. Konkel, "Abrasive Wear-Microstructure Interactions in a Ni-Cr White Iron," submitted to Wear.

2. W. L. Silence, "Effect of Structure on Wear Resistance of Co-, Fe-, and Ni-Base Alloys," J. Lubrication Tech., 100 (1978) pp. 428-435.

3. R. J. Dawson, S. Shewchuck, and R. A. Beland, "Using Abrasion Test Data to Select Hardfacing and Build-Up Materials for a Hammermill," paper presented at the 17th Annual Conference of Metallurgists - CIM, Montreal, August 1978.

4. K. H. Zum-Gahr, "Relation Between Abrasive Wear Rate and the Microstructure of Metals," pp. 266-274, proceedings of The International Conference on Wear of Materials, ASME, Dearborn, Michigan, April 1979.

5. J. Larsen-Badse, "The Abrasion Resistance of Some Hardened and Tempered Carbon Steels," Trans. AIME, 236 (1966) pp. 1461-1466.

6. J. Larsen-Badse, "Abrasion Resistance of Some S.A.P.-Type Alloys at Room Temperature," Wear, 12 (1968) pp. 357-368.

7. F. T. Furillo, "W-Mo Carbides for Hard Facing Applications," pp. 415-426, proceedings of The International Conference on Wear of Materials, ASME, Dearborn, Michigan, April 1979.

8. E. Rabinowicz, Friction and Wear of Materials, p. 168; Wiley, New York, 1965.

9. M. J. Murray, P. J. Mutton, and J. D. Watson, "Abrasive Wear Mechanisms in Steels," pp. 257-265, proceedings of The International Conference on Wear of Materials, ASME, Dearborn, Michigan, April 1979.

10. T. O. Mulhearn and L. E. Samuels, "The Abrasion of Metals: A Model of the Process," Wear, 5 (1962) pp. 478-498.

11. J. Larsen-Badse, "Influence of Grit Size on the Groove Formation During Sliding Abrasion," Wear, 11 (1968) pp. 213-222.

12. J. Larsen-Badse, "Influence of Grit Diameter and Specimen Size on Wear During Sliding Abrasion," Wear, 12 (1968) pp. 35-53.

13. H. S. Avery, "Classification and Precision of Abrasion Tests," pp. 148-157, proceedings of The International Conference on Wear of Materials, ASME, St. Louis, Missouri, April 1977.

14. Private communication, P. Swanson, Deere & Co. Technical Center, Moline, Illinois, July 1979.

DISTRIBUTION LIST

Mr. John J. Mahoney
Senior Contract Administrator
Contracts Management Office
DOE- Chicago Operations Office
9700 South Cass Avenue
Argonne, IL 60439
- 6 copies -

Dr. S. J. Dapkunas
Division of System Engineering/
Energy Technology
U.S. D.O.E.
Room C-155
Germantown, MD 21401
- 3 copies -

Dr. Paul Scott
Division of System Engineering/
Energy Technology
U.S. D.O.E.
Room C-155
Germantown, MD 21401

Dr. Sam Schneider
National Bureau of Standards
Washington, D.C. 20234

Dr. John Dodd
Climax Molybdenum Company
13949 West Colfax Avenue
Golden, CO 80401

Metals and Ceramics Information Center
Battelle-Columbus Laboratories
505 King Avenue
Columbus, OH 43201

Mr. D. Doane
Climax Molybdenum Research Lab
1600 Huron Parkway
Ann Arbor, MI 48106

Dr. M. S. Bhat
Materials and Molecular Research Div.
Bldg. 62 - Room 239
Lawrence Berkeley Laboratory
University of California
Berkeley, CA 94720

Mr. Howard Avery
69 Alcott
Mahwah, N.J. 07430

Dr. Kenneth Antony
Stellite Division
Cabot Corporation
Kokomo, IN 46901

Dr. Stanley Wolf
Materials Science Program
Basic Energy Sciences Division
D.O.E.
Washington, D.C. 20545

Dr. Joseph Klein
Stellite Division
Cabot Corporation
Kokomo, IN 46901

Dr. Jerry L. Arnold
Research and Technology
Armco Steel Corporation
Middletown, OH 45043

Dr. R. D. Tucker
Union Carbide Corp.
1500 Polco Street
Indianapolis, IN 46224

Dr. Paul Swanson
Deere and Company Technical Center
3300 River Drive
Moline, IL 61265

Dr. Jeffrey S. Hansen
P.O. Box 70
Bureau of Mines
Albany, OR 97321

Dr. R. J. Dawson
Falconbridge Nickel Mines Ltd.
P.O. Box 900, 8810 Yonge Street
Thornhill, Ontario, Canada L3T 4A8

Dr. Burton R. Patterson
Southern Research Institute
2000 Ninth Avenue, South
Birmingham, AL 35205

Dr. S. Shankar
Technical Center
Howmet Turbine Components Corp.
699 Benston Road
Whitehall, MI 49461

Dr. Martin A. Moore
Fulmer Research Institute Limited
Stoke Pages, Slough
SL2 4QD
England